Transverse momentum fluctuations in ultrarelativistic Pb + Pb and p + Pb collisions with "wounded" quarks

Piotr Bożek[1,*] and Wojciech Broniowski[2,3,†]

[1]*AGH University of Science and Technology, Faculty of Physics and Applied Computer Science, al. Mickiewicza 30, 30-059 Cracow, Poland*
[2]*The H. Niewodniczański Institute of Nuclear Physics, Polish Academy of Sciences, 31-342 Cracow, Poland*
[3]*Institute of Physics, Jan Kochanowski University, 25-406 Kielce, Poland*

We analyze the phenomenon of size-flow transmutation in ultrarelativistic nuclear collisions in a model where the initial size fluctuations are driven by the wounded quarks and the collectivity is provided by viscous hydrodynamics. It is found that the model properly reproduces the data for the transverse momentum fluctuations measured for Pb+Pb collisions at $\sqrt{s_{NN}} = 2.76$ TeV by the ALICE Collaboration. The agreement holds for a remarkably wide range of centralities, from 0–5 % up to 70–80 %, and displays a departure from a simple scaling with $(dN_{\mathrm{ch}}/d\eta)^{1/2}$ in the form seen in the data. The overall agreement in the model with wounded quarks is significantly better than with nucleon participants. This feature joins the previously found wounded quark multiplicity scaling in the argumentation in favor of subnucleonic degrees of freedom in the early dynamics. We also examine in detail the correlations between measures of the initial size and final average transverse momentum of hadrons. Predictions are made for the transverse momentum fluctuations in p+Pb collisions at $\sqrt{s_{NN}} = 5.02$ TeV.

I. INTRODUCTION

Collectivity of the intermediate evolution of fireballs created in ultrarelativistic nuclear collisions is by now a well-accepted fact, allowing, in particular, for a qualitative and quantitative understanding of harmonic flow phenomena as due to the initial transverse shape which fluctuates event by event. It is somewhat less commonly known that the same underlying physical effects (initial fluctuations and collectivity) jointly lead to sizable event-by-event transverse momentum fluctuations, one of the basic observables studied from the outset of the relativistic collisions program. The pertinent *size-flow transmutation* effect was brought up for the first time in Ref. [1] and further elaborated in Ref. [2], where we presented a detailed study comparing a 3+1-dimensional (3+1D) viscous hydrodynamic simulations to the data from the BNL Relativistic Heavy-Ion Collider (RHIC).

In this paper we extend the analysis of Ref. [2] by passing to subnucleonic degrees of freedom, namely, the wounded quarks [3,4], in modeling of the initial stage. We show that the approach leads to a surprisingly accurate description of the recent data [5] from the CERN Large Hadron Collider (LHC) for Pb+Pb collisions at $\sqrt{s_{NN}} = 2.76$ TeV, holding in a very wide range of the collision centralities, from 0–5 % to 70–80 %. Passing to subnucleonic components is physically desirable for other reasons, as it allows for a natural scaling of the multiplicity of produced hadrons on the number of (subnucleonic) participants (for a compilation of results see, e.g., [6,7]). Importantly, the results for the shape eccentricities are similar with wounded quarks [7] to models based on nucleon participants, whereby the successful phenomenology

of the harmonic flow obtained with wounded nucleon initial conditions is maintained.

Since the transverse momentum fluctuations reveal relevant details of the early dynamics of the system formed in ultrarelativistic nuclear collisions, they have been intensely investigated both theoretically [8–29] and experimentally [5,30–38].

From a broader perspective, the analysis presented in this paper contributes to the discussion of the nature of the initial stage, its degrees of freedom and fluctuations; the results are also to some extent sensitive to properties of the intermediate evolution (hydrodynamics, transport). Comparisons to present and future data, made jointly with other observables, may help to resolve the issue. We also make predictions for the transverse momentum fluctuations in p+Pb collisions at $\sqrt{s_{NN}} = 5.02$ TeV, which can be tested in future data analyses.

II. BASIC INGREDIENTS

A. Size-flow transmutation

We begin with a reminder of the size-flow transmutation phenomenon [1,2]. When two nuclei collide, the number of participants and the transverse size of the fireball fluctuate. Even when we take a subsample with exactly the same number of participants, the size is slightly (a few percent) different from event to event. The amount of these fluctuations depends on a specific model of the nucleon structure and elementary collisions, but the effect persists as a generic phenomenon. If two fireballs created with the same number of participants (thus having nearly equal entropy) have different size, then the smaller one will lead to faster collective expansion (cf. Fig. 1). In hydrodynamics this is caused by a larger radial gradient of the pressure, whereas in transport models by a higher collision rate of partons. As a result, the smaller system leads to a larger radial flow, and consequently, a larger average

---

*Piotr.Bozek@fis.agh.edu.pl
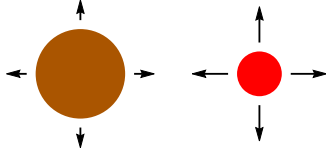†Wojciech.Broniowski@ifj.edu.pl

FIG. 1. A cartoon view of the size-flow transmutation effect. If two fireballs of equal entropy differ in size, a smaller one will lead via collective evolution to a stronger radial flow [1].

transverse momentum in the event, denoted as $\langle p_T \rangle$. Thus, on these general grounds, we expect a strong negative correlation between the initial fireball size and $\langle p_T \rangle$.

B. Wounded quarks

The concept of wounded quarks in the Glauber-motivated approach [39,40] to inelastic production in the early phase of the collision was developed in [3,4] shortly after the proposal of wounded nucleons [41] (for a review see [42]). Over the years it has been argued [6,7,43–51] that the wounded quarks lead to a more natural description of the multiplicity of produced hadrons, with the simple scaling

$$\frac{dN_{\mathrm{ch}}}{d\eta} \sim Q_{\mathrm{W}}, \tag{1}$$

where Q_{W} denotes the number of wounded quarks. The scaling holds to a very reasonable accuracy for a variety of reactions, including $p + p$ collisions, and centralities [7], with the proportionality constant dependent only on $\sqrt{s_{NN}}$. The quality of scaling improves with increasing collision energy. The key role of the subnucleonic constituents such as the wounded quarks lies in enhanced combinatorics. We note that intermediate combinatorics of the quark-diquark model [52] also leads to a correct description of the RHIC data as well as the proton-proton elastic scattering amplitude at the energies of the CERN Intersecting Storage Rings (ISR).

Our previous study [2] involved the wounded nucleon model, amended with binary collisions [53] (the so-called *mixed* model),

$$\frac{dN_{\mathrm{ch}}}{d\eta} \sim \frac{1-a}{2} N_{\mathrm{W}} + a N_{\mathrm{bin}}, \tag{2}$$

where N_{W} and N_{bin} denote the number of wounded nucleons the number of binary collisions, respectively. The binary component is crucial for the description of the experimental data [54]. With a suitable choice of the mixing parameter a (at the LHC energies $a \simeq 0.15$) the model (2) is capable of explaining the multiplicity distribution at RHIC and the LHC in a hydrodynamic approach [55]. However, importantly for the message of the present work, the initial conditions for hydrodynamics generated with the mixed model lead to sizably (by about 50%) too large transverse momentum fluctuations for the most central collisions [2].

We remark that the wounded quarks may be regarded in more general terms of partonic degrees of freedom and generalized to more than three constituents [7,51]. The active constituents (those emitting to the midrapidity region) may also be interpreted in terms of partonic hot-spots (see, e.g.,

[56,57]). As these hot-spots are gluonic in the origin, their number is a free parameter, not linked to the number of quarks. Interpretation based on QCD modeling suggests that at the midrapidity region in ultrarelativistic collisions the gluonic degrees of freedom play a dominant role, hence the potential role of gluonic hot-spots.

C. Measures of the initial size

The initial transverse profiles of the fireball are obtained with the implementation of the wounded quark model in GLISSANDO [58], as described in detail in Ref. [7]. Here we only stress that care has been taken to distribute quarks within the nucleon in such a way that the charge rms radius of the proton agrees with the experimental values, as well as to reproduce the nucleon-nucleon inelasticity profile and the inelastic NN cross section, which are accessible experimentally. The result of GLISSANDO is the transverse distribution of point-like sources, which then are smeared with a Gaussian of width of 0.3 fm in the case of wounded quarks and 0.4 fm in the case of the wounded nucleons. Such a smearing is physically motivated and must always be done in applications of the Glauber modeling of the initial conditions for use in hydrodynamics. Admittedly, the smearing parameter influences the eccentricity measures, and its increase smoothes out the distributions whereby reducing the harmonic eccentricity moments.

Denoting thus obtained initial transverse entropy profile in event k as $s_k(x,y)$, we may define several measures of its transverse extent. The simplest one is the rms radius of a single event,

$$\langle r^2 \rangle = \frac{\int dx\, dy\, s_k(x,y)(x^2+y^2)}{\int dx\, dy\, s_k(x,y)}, \tag{3}$$

$$\langle r \rangle_k \equiv \sqrt{\langle r^2 \rangle}.$$

Averaging over N_{ev} events is denoted with another pair of brackets, for instance the event-averaged transverse size is denoted as

$$\langle\langle r \rangle\rangle = \frac{1}{N_{\mathrm{ev}}} \sum_{k=1}^{N_{\mathrm{ev}}} \langle r \rangle_k. \tag{4}$$

For sources with a large azimuthal deformation, a definition of the size parameter more appropriate for large asymmetries has been proposed in Ref. [59]:

$$\frac{1}{\bar{R}} = \sqrt{\frac{1}{\sigma_x^2} + \frac{1}{\sigma_y^2}}, \tag{5}$$

where $\sigma_{x,y}$ denote the widths of the fireball density along its principal axes.

D. 3+1D viscous hydrodynamics and statistical hadronization

In our study we use the 3+1D event-by-event viscous hydrodynamics [60]. The details of the approach have been presented in Ref. [2]. As previously, we use constant shear viscosity to entropy density (s) ratio $\eta/s = 0.08$, constant bulk viscosity to s ratio $\zeta/s = 0.04$ (present only in the hadronic phase), whereas the corresponding relaxation times are

$\tau_\pi = 3\eta/(Ts)$ and $\tau_\Pi = \tau_\pi$. The hydrodynamic evolution is started at the time $\tau_0 = 0.6$ fm/c. The equation of state interpolates between the lattice-QCD results at high temperatures [61] and a hadron gas at low temperatures [62,63].

To carry out the statistical Cooper-Frye [64] hadronization at the freeze-out temperature $T_f = 150$ MeV we run THERMINATOR [65,66], which includes resonance decays of all hadrons listed in the Particle Data Tables. That way we simulate events in a close resemblance to the experiment, with the kinematic cuts as in the pertinent ALICE analysis of Ref. [5]: $|\eta| < 0.8$ for the pseudorapidity and $0.15 < p_T < 2$ GeV for the transverse momentum of the registered hadrons.

Event-by-event hydrodynamic simulations with fluctuating initial conditions have been performed for perfect fluid and for the viscous case, focusing on collective flow (for reviews, see [67–69]).

E. Measure of the transverse momentum fluctuations

Since the events consist of a large but finite number of hadrons, the p_T fluctuations involve a trivial component coming from sampling of particles at the freeze-out hypersurface with a limited multiplicity. Even if the conditions at freeze-out were exactly the same in each event, we would get this spurious effect. Many statistical measures have been designed to get rid of the trivial fluctuations. In our study we use a measure proposed by the STAR Collaboration [35]:

$$\langle \Delta p_T \Delta p_T \rangle \equiv \frac{1}{N_{\text{ev}}} \sum_{k=1}^{N_{\text{ev}}} \frac{C_k}{N_k(N_k - 1)} \quad (6)$$

with N_k denoting the multiplicity in event k and

$$C_k = \sum_{i=1}^{N_k} \sum_{j=1, j \neq i}^{N_k} (p_{Ti} - \langle\!\langle p_T \rangle\!\rangle)(p_{Tj} - \langle\!\langle p_T \rangle\!\rangle), \quad (7)$$

where

$$\langle\!\langle p_T \rangle\!\rangle = \frac{1}{N_{\text{ev}}} \sum_{k=1}^{N_{\text{ev}}} \langle p_T \rangle_k. \quad (8)$$

In Ref. [2] we have shown that the measure may be more conveniently rewritten as

$$v\langle \Delta p_T \Delta p_T \rangle = \frac{N_{\text{ev}} - 1}{N_{\text{ev}}} \text{var}(\langle p_T \rangle) - \frac{1}{N_{\text{ev}}} \sum_{k=1}^{N_{\text{ev}}} \frac{\text{var}_k(p_T)}{N_k}, \quad (9)$$

which explicitly displays a difference of two terms: the variance of the mean transverse momenta in events, and the event-averaged variance of the transverse momentum in each event divided by its multiplicity. A technical simplification is that Eq. (9) involves only single and not double sums in the event, which facilitates the computations.

What is used in our comparisons to the data is the scaled measure $\langle \Delta p_T \Delta p_T \rangle^{1/2}/\langle\!\langle p_T \rangle\!\rangle$.

III. COMPARISON TO THE ALICE DATA

We start presenting our results with Fig. 2, where we compare $\langle \Delta p_T \Delta p_T \rangle^{1/2}/\langle\!\langle p_T \rangle\!\rangle$ obtained with simulations described
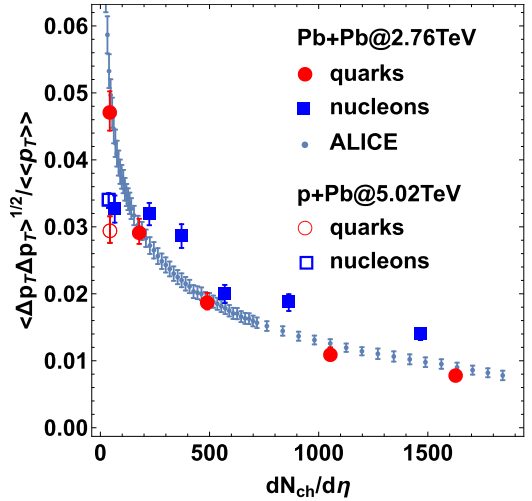

FIG. 2. The STAR measure of the transverse momentum fluctuations plotted vs charged hadron multiplicity. The simulations with the wounded quarks and nucleons are described in the text. The filled symbols correspond to the case of Pb+Pb collisions, whereas the empty symbols indicate our predictions for p+Pb collisions at centrality 0–3 %. The experimental data for Pb+Pb case come from the ALICE Collaboration [5].

in Sec. II to the experimental data. We use two models of the initial state: the wounded quark model of Eq. (1) and the mixed nucleon model of Eq. (2). The experimental data for Pb+Pb collisions at $\sqrt{s_{NN}} = 2.76$ TeV come from the ALICE Collaboration [5]. We note that the achieved agreement of the wounded quark model (circles) with the data is remarkable and extends over the whole multiplicity range, from central collisions (our right-most point corresponds to centrality 0–5 %) to peripheral collisions of centrality 70–80 %. This agreement is nontrivial, as a similar simulation but with the nucleon participants in the initial state is not nearly as good (squares): In this case, at highest multiplicities the data are overshot by about 50%, whereas at low multiplicities the nucleon model predictions fall below the experiment.

We note that in the quark case the nontrivial experimental dependence on $dN_{\text{ch}}/d\eta$ is reproduced. As already pointed out in Ref. [5], this dependence does not follow a simple scaling with $(dN_{\text{ch}}/d\eta)^{-1/2}$, which precludes the interpretation in terms of independent superposition of nucleon-nucleon collisions. For a better visualization of this issue, in Fig. 3(a) we show the result in the log-log scale. It can be clearly seen that the slope changes non-monotonically with the multiplicity, assuming largest negative values for most central collisions, then slightly flattening out, to increase a bit again for peripheral collisions. The same feature may be be read out from Fig. 3(b), where following Ref. [5] we examine the ratio $\langle \Delta p_T \Delta p_T \rangle^{1/2}/[\langle\!\langle p_T \rangle\!\rangle (dN_{\text{ch}}/d\eta)^{-1/2}]$, which is the relative slope with respect to the independent superposition case.

In Figs. 2 and 3 we also present our predictions for the p+Pb collisions at the LHC (empty symbols) for multiplicities corresponding to a high centrality 0–3 %. We recall that in such high-multiplicity collisions collectivity is expected to
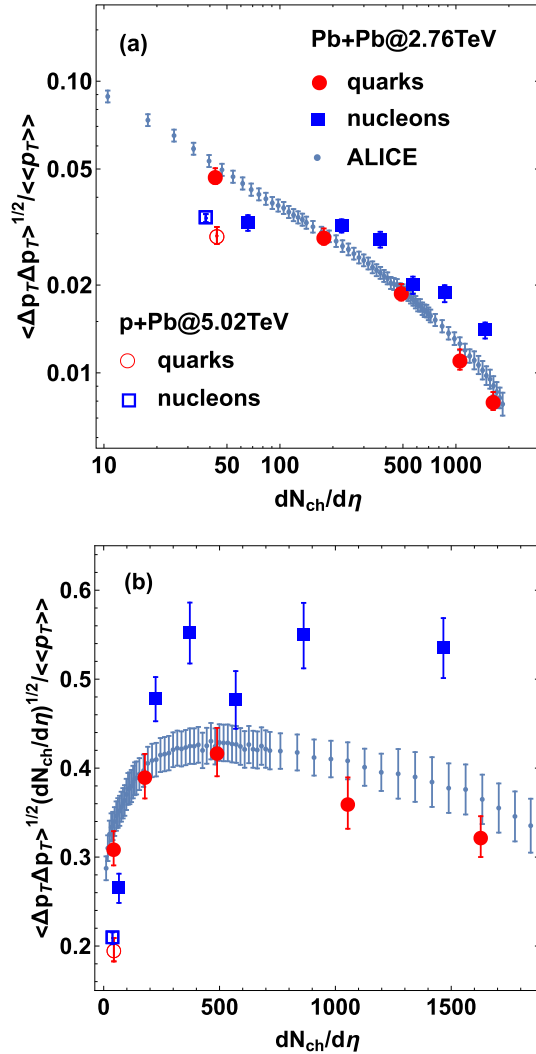
FIG. 3. The same as Fig. 2 but (a) plotted in the log-log scale and (b) for the ratio $\langle \Delta p_T \Delta p_T \rangle^{1/2}/[\langle\langle p_T \rangle\rangle (dN_{ch}/d\eta)^{-1/2}]$ plotted in the log-linear scale.

develop and hydrodynamic description leads to appropriate phenomenology even in small systems (e.g., see Ref. [70]). These results may be confronted with future data analyses.

IV. UNDERSTANDING THE RESULTS

This section is devoted to the understanding of the mechanism standing behind the agreement of the wounded quark+hydro approach exhibited in Figs. 2 and 3. The following discussion does not affect *per se* the results of the previous section, which were obtained in a robust way by just running the simulations, but it provides an interesting insight into the behavior of hydrodynamics, in particular, its response to the initial conditions.

A. Initial size–transverse momentum correlations

Generally, the obtained results depend on the fluctuations in the initial condition and on their transmutation to the radial flow fluctuations by hydrodynamics. In the following we
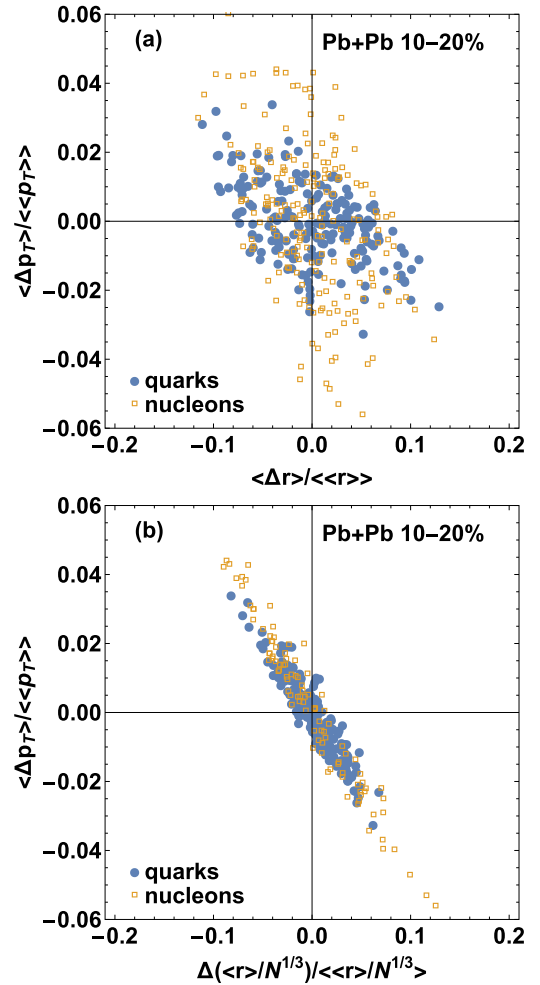

FIG. 4. Scattered plot illustrating the correlation of the initial size and the transverse momentum in events for Pb+Pb collisions in 10–20 % centrality bin. The results for the calculation using quark and nucleon Glauber models are denoted with filled circles and empty squares, respectively. (a) shows the correlation between the r.m.s. radius and the average transverse momentum in an event. (b) displays the correlation between the rescaled rms radius and the average transverse momentum.

explore in detail how the size-flow transmutation is realized in our hydrodynamic approach and also to what extent the size estimator of Eq. (3) is universal in the sense that in a class of events with the same value of $\langle r \rangle$ (which otherwise may differ in shape or other radial moments) the resulting value of $\langle p_T \rangle$ is similar. To check it, we have generated scattered plots shown in Fig. 4(a), where we plot $\langle \Delta r \rangle$ vs $\langle \Delta p_T \rangle$, defined in event k as

$$\langle \Delta r \rangle_k = \langle r \rangle_k - \langle\langle r \rangle\rangle, \quad \langle \Delta p_T \rangle_k = \langle p_T \rangle_k - \langle\langle p_T \rangle\rangle. \quad (10)$$

In this comparison the average transverse momentum for a given event is calculated by sampling the Cooper-Frye emission with a very large multiplicity (100–2000 times the real event multiplicity). With such an oversampling, the obtained values of the average transverse momentum in the event have
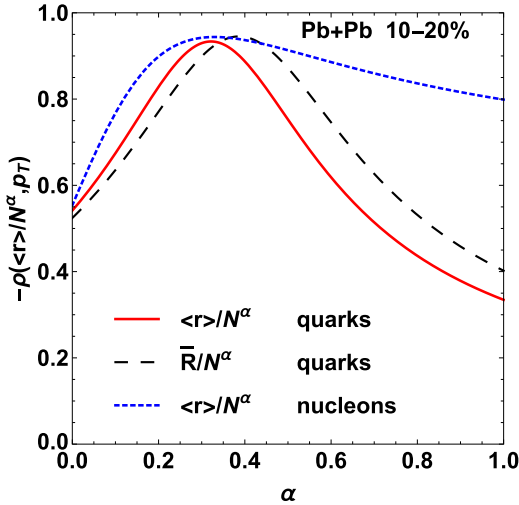
FIG. 5. Dependence of the anticorrelation between the rescaled fireball size $\langle r \rangle / N^\alpha$ and the average $\langle p_T \rangle$ in the event on the scaling power α for 10–20 % centrality Pb+Pb collisions.

a negligible component related to the finite multiplicity [the last term in Eq. (9)], which simplifies the comparison.

Before further discussion, let us mention a rather technical issue which will, however, lead to interesting conclusions. Our samples correspond to centrality classes with the standard widths of 5% for the most central and 10% for more peripheral collisions. Within such rather wide bins, necessary for sufficient statistics, the multiplicity of events fluctuates. One trivially expects that on the average larger size fireballs will also ultimately produce more hadrons. To remove this trivial effect of centrality fluctuations one should take narrow centrality classes, as was possible in the experiment [5]. Our limited statistics does not allow for this remedy, however, one can resort to another method. We find that in the applied Glauber model [58] the increase of the average fireball size with the number of participants scales approximately as $\langle r \rangle \propto N^{0.2-0.5}$. It means that within a given centrality class a large part of the size variation comes from a change in the initial entropy. We improve the size measure of Eq. (3) by scaling it with a power of the entropy in the event (or a related measure such as the number of wounded participants),

$$\langle r \rangle_k \to \langle r \rangle_k / N_k^\alpha, \qquad (11)$$

where α is a numerically adjusted parameter. In Fig. 5 we display the correlation coefficient between $\langle \Delta r \rangle / N^\alpha$ and $\langle \Delta p_T \rangle$ for events in the 10–20 % centrality class as a function of α. Both for the models with quark and nucleon participants a maximum correlation occurs for $\alpha \simeq 1/3$ (dashed and dashed-dotted lines in Fig. 5). We have also tested the correlation in the case when the size is estimated using the asymmetric variable $\bar{R}$ of Eq. (5). In all the cases the correlation is strongest around $\alpha = 0.3–0.4$, with similar values of the correlation coefficient. For the calculation with the quark Glauber model the value of α where the correlation is maximal changes weakly with centrality, whereas for the nucleon model it increases up to $\alpha \simeq 0.42$ in peripheral collisions.

The estimator of Eq. (11) works much better than the standard definition of Eq. (3), as can be promptly seen from panel (b) in Fig. 4. The improvement occurs for both the wounded quark model (filled symbols) and the nucleon case (empty symbols). We have checked the the rescaled estimator yields a much stronger correlation with the final transverse momentum for all centralities in Pb+Pb and for central p+Pb collisions.

The rescaled radius (11) is very similar to the estimator of the strength of the subleading component in the principal component analysis of the transverse momentum spectra by Mazeliauskas and Teaney [71], who use as an estimator the combination

$$\langle \Delta p_T \rangle \propto \beta \epsilon_{0,0} + \epsilon_{0,2}, \qquad (12)$$

where

$$\epsilon_{m,n} e^{im\Psi_{m,n}} = -\frac{\int dx\, dy\, s_k(x,y)(x^2 + y^2)^{n/2} e^{im\phi}}{\langle \int dx\, dy\, s_k(x,y) \rangle \langle\langle r \rangle\rangle^{n/2}}. \qquad (13)$$

For the calculation in the wounded quark model we find that the largest correlation with the transverse momentum with the estimator (12) occurs for $\beta \simeq -5/3$. To linear order in deviations from average values in the centrality bin, this is equivalent to the rescaled rms radius (11) with $\alpha \simeq 1/3$.

The anticorrelation coefficient for the estimator $\langle r \rangle / N^\alpha$ and for the linear combination $\beta \epsilon_{0,0} + \epsilon_{0,2}$ is displayed in Fig. 6 for the initial state given by the quark [panel (a)] and nucleon [panel (b)] models. For both models we notice that the estimator $\langle r \rangle / N^\alpha$ and the estimator (12) give very similar results, as expected. Quantitatively, the two models have different correlations. In the nucleon model the anticorrelation is very strong for all centralities. In the quark model for the most central collisions the anticorrelation is essentially perfect, with the correlation coefficient very close to -1. It gradually increases to about -0.6 at $c = 80\%$. Estimators based on $\bar{R}$ yield similar results.

In the quark Glauber model used in our calculation the eccentricity is larger that in its nucleon version. This may indicate the need to include higher harmonic moments in the estimator, e.g., the second harmonic moment $\epsilon_{2,2}$ is up 60% larger in the quark model in peripheral collisions. A significant improvement in the quality of the estimator for the quark model is visible when using a formula including initial eccentricity [diamonds in Fig. 6(a)]

$$\langle \Delta p_T \rangle \propto \beta \epsilon_{0,0} + \epsilon_{0,2} + \gamma \epsilon_{2,2}. \qquad (14)$$

With the two-parameter estimator (14), the anticorrelation with the final momentum is strong except for the most peripheral bin. The use of this more general formula gives no significant improvement in the prediction of the final $\langle p_T \rangle$ for the nucleon model [diamonds in Fig. 6(b)].

B. Size fluctuations in the initial state

We now present a closer look at the systematics of the initial condition generated in our approach with GLISSANDO [58]. We also explore a potentially relevant ingredient, namely, the possible additional fluctuations in the initial state. The idea here is based on an intuitive expectation that an elementary
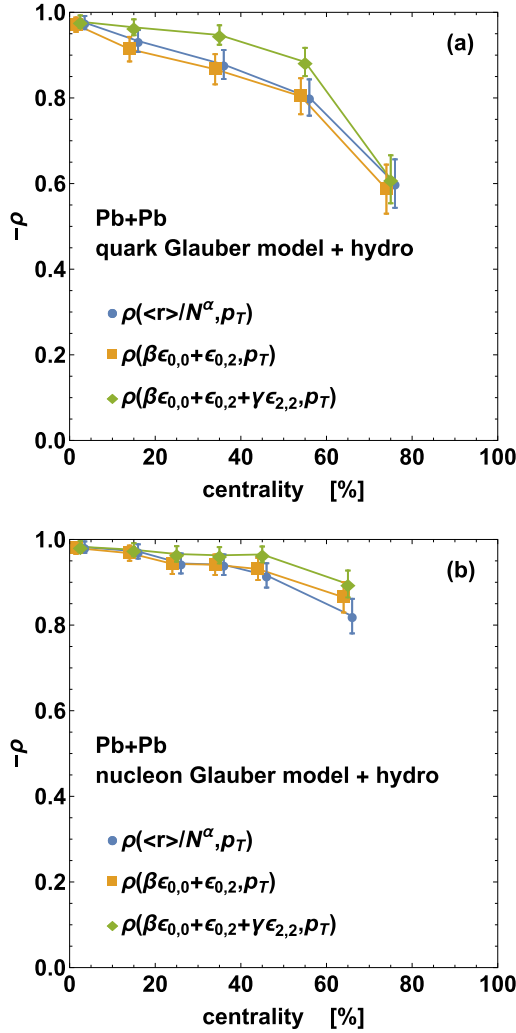
FIG. 6. Event-by-event anticorrelation coefficient of the estimators of size described in the text and the transverse momentum $\langle p_T \rangle$, plotted versus the centrality of the collision.

FIG. 7. Size fluctuations plotted as functions of centrality in various models of the initial state. Label "quarks" refers to the wounded quark model (thick lines) and "nucleons" to the mixed nucleon model (thin lines). Γ indicates an overlayed Γ distribution with parameter κ. See text for further details.

collision need not always deposit the same amount of entropy, but the quantity may fluctuate. In fact, in small systems such fluctuations are needed to describe the multiplicity fluctuations of the produced hadrons. In Ref. [58] we have proposed that the strength of the Glauber sources should fluctuate according to the Γ distribution, which then upon folding with the Poissonian distribution due to hadronization and detector acceptance, yields the negative binomial distribution, efficient in fitting the data. It is not *a priori* clear how much of these extra fluctuations should be present in the initial state in the $A + A$ collisions. The parameter which controls their magnitude is κ, which equals to the ratio of the mean squared to the variance of the Γ distribution of the source strengths.

The results are shown in Fig. 7, where we plot the scaled standard deviation of the transverse size given by Eq. (3) as a function of centrality. We show the outcome of the simulations for the wounded quark model (thick lines) and for the mixed nucleon model (thin lines). Very narrow centrality bins are determined independently for each model variant, such that the results can be compared in a uniform way. We note
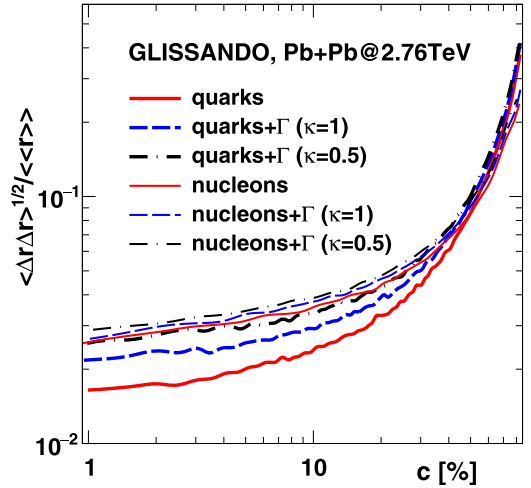
several facts. First, size fluctuations from the wounded quark model without additional fluctuations are, at low centralities, significantly below the nucleon model. This explains the fact that the hydrodynamic simulations with the wounded quark initial condition (without extra fluctuations) presented in Sec. III work well, as opposed to the nucleon case. Second, increasing the overlaid fluctuations (by decreasing the value of κ) leads to increased size fluctuations, as intuitively expected. With fluctuations included, the results for the wounded quark model increase, approaching the mixed nucleon model range at $\kappa \sim 0.5$. That would of course spoil the agreement with the data shown in Fig. 2.

We recall that to reproduce the multiplicity fluctuations in $p + $Pb collisions in the wounded quark model at very large average multiplicities (the tail of the distribution), one needs to overlay a distribution with small κ, of the order of 0.5. Thus it seems impossible to describe in a uniform way the $p + $Pb high-multiplicity data and the Pb+Pb transverse momentum fluctuations. One should bare in mind, however, that the ultracentral $p + $Pb collisions may involve different physical mechanisms. The problem requires a deeper understanding and further studies.

C. Insensitivity to variants of hadronization

In a final check we show a remarkable insensitivity of our simulations to models of hadronization. In Fig. 8 we show the results from a standard THERMINATOR hadronization model taking into account charged pions, kaons, protons, and antiprotons after decays of all resonances (circles), from a model which incorporates late charge balancing as implemented in Ref. [72] (up triangles), and from the primordial (before resonance decays) charged pions, kaons, protons and antiprotons (down triangles). The near-equality of all variants reflects the robustness of the STAR correlation measure applied in our analysis.
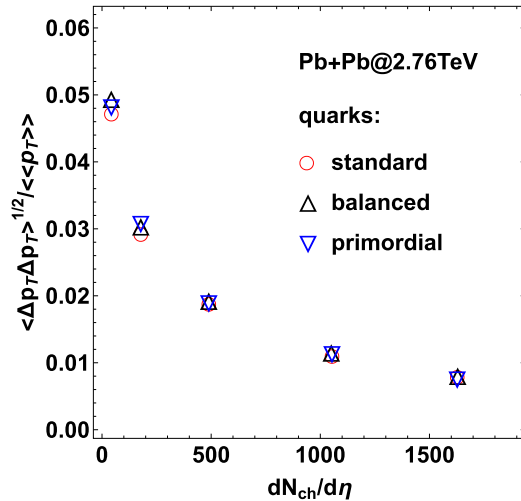
FIG. 8. Same as in Fig. 2 for the wounded quark case with various models of hadronization.

V. CONCLUSIONS

Fluctuations of the average transverse momentum of particles emitted in relativistic heavy-ion collisions are calculated using a viscous hydrodynamic model. Event-by-event fluctuations of the fireball lead to event-by-event fluctuations of the average transverse momentum. The initial state obtained in the Glauber Monte Carlo model with quark degrees of freedom describes properly the $\langle p_T \rangle$ fluctuations in Pb+Pb collisions measured by the ALICE Collaboration. The data are well described in a wide range of centralities, from 0–5 % to 70–80 %. On the other hand, the calculation using the initial state with nucleon degrees of freedom overestimates the observed data at central collisions. The dependence of the experimentally observed fluctuations on centrality departs

from the simple scaling $(dN_{ch}/d\eta)^{-1/2}$, holding for the independent superposition model. This nontrivial centrality dependence is well described by our calculation. Predicted momentum fluctuations in p+Pb collisions are smaller than in Pb+Pb collisions at the same multiplicity of produced charged hadrons.

The average transverse flow in an event is correlated with the initial rms radius scaled by a power of the initial entropy. We confirm the results of Ref. [71] that this correlations is almost perfect in the model with nucleon degrees of freedom. In the calculation using the wounded quark model the correlation is somewhat weaker. An improvement of the correlations of the estimators with the final transverse momentum is possible adding a term to the estimator formula with the initial eccentricity.

The comparison of model results using primordial particles, particles including resonance decay products, or the calculation with imposed late-stage local charge conservation effects show that the resulting effects are very small in transverse momentum fluctuations. However, other sources of fluctuations can increase the observed $\langle p_T \rangle$ fluctuations. We show that additional fluctuations in the entropy deposition in the initial state may give rise to a significant increase of $\langle p_T \rangle$ fluctuations. The measurements of the ALICE Collaboration can thus provide an upper bound on the the strength of such entropy fluctuations in the initial state.

[1] W. Broniowski, M. Chojnacki, and L. Obara, Phys. Rev. C **80**, 051902(R) (2009).

[2] P. Bożek and W. Broniowski, Phys. Rev. C **85**, 044910 (2012).

[3] A. Białas, W. Czyż, and W. Furmański, Acta Phys. Pol. B **8**, 585 (1977); A. Białas, K. Fiałkowski, W. Słomiński, and M. Zieliński, *ibid.* **8**, 855 (1977); A. Białas and W. Czyż, *ibid.* **10**, 831 (1979).

[4] V. V. Anisovich, Yu. M. Shabelski, and V. M. Shekhter, Nucl. Phys. B **133**, 477 (1978).

[5] B. B. Abelev *et al.* (ALICE Collaboration), Eur. Phys. J. C **74**, 3077 (2014).

[6] R. A. Lacey, P. Liu, N. Magdy, M. Csand, B. Schweid, N. N. Ajitanand, J. Alexander, and R. Pak, arXiv:1601.06001.

[7] P. Bożek, W. Broniowski, and M. Rybczyński, Phys. Rev. C **94**, 014902 (2016).

[8] M. Gazdzicki and S. Mrowczynski, Z. Phys. C **54**, 127 (1992).

[9] L. Stodolsky, Phys. Rev. Lett. **75**, 1044 (1995).

[10] E. V. Shuryak, Phys. Lett. B **423**, 9 (1998).

[11] S. Mrowczynski, Phys. Lett. B **430**, 9 (1998).

[12] F. Liu, A. Tai, M. Gazdzicki, and R. Stock, Eur. Phys. J. C **8**, 649 (1999).

[13] S. A. Voloshin, V. Koch, and H. G. Ritter, Phys. Rev. C **60**, 024901 (1999).

[14] G. Baym and H. Heiselberg, Phys. Lett. B **469**, 7 (1999).

[15] S. A. Voloshin (STAR Collaboration), AIP Conf. Proc. **610**, 591 (2001).

[16] R. Korus, S. Mrowczynski, M. Rybczyński, and Z. Wlodarczyk, Phys. Rev. C **64**, 054908 (2001).

[17] S. Gavin, Phys. Rev. Lett. **92**, 162301 (2004).

[18] J. Dias de Deus, E. Ferreiro, C. Pajares, and R. Ugoccioni, Eur. Phys. J. C **40**, 229 (2005).

[19] S. A. Voloshin, Nucl. Phys. A **749**, 287 (2005).

[20] S. Mrowczynski, M. Rybczyński, and Z. Wlodarczyk, Phys. Rev. C **70**, 054906 (2004).

[21] M. Abdel-Aziz and S. Gavin, Nucl. Phys. A **774**, 623 (2006).

[22] W. Broniowski, B. Hiller, W. Florkowski, and P. Bożek, Phys. Lett. B **635**, 290 (2006).

[23] D. J. Prindle and T. A. Trainor (STAR Collaboration), PoS **CFRNC2006**, 007 (2006).

[24] S. Gavin and M. Abdel-Aziz, Phys. Rev. Lett. **97**, 162302 (2006).

[25] M. Sharma and C. A. Pruneau, Phys. Rev. C **79**, 024905 (2009).

[26] S. Mrowczynski, Acta Phys. Pol. B **40**, 1053 (2009).

[27] Y. Hama, R. P. G. Andrade, F. Grassi, W. L. Qian, and T. Kodama, Acta Phys. Pol. B **40**, 931 (2009).

[28] T. A. Trainor, Phys. Rev. C **92**, 024915 (2015).

[29] Q. Liu and W.-Q. Zhao, arXiv:1611.02532.

[30] J. Adams *et al.* (STAR Collaboration), Phys. Rev. C **71**, 064906 (2005).

[31] D. Adamova *et al.* (CERES Collaboration), Nucl. Phys. A **727**, 97 (2003).

[32] S. Adler *et al.* (PHENIX Collaboration), Phys. Rev. Lett. **93**, 092301 (2004).

[33] T. Anticic *et al.* (NA49 Collaboration), Phys. Rev. C **70**, 034902 (2004).

[34] J. Adams *et al.* (STAR Collaboration), J. Phys. G **34**, 799 (2007).

[35] J. Adams *et al.* (STAR Collaboration), Phys. Rev. C **72**, 044902 (2005).

[36] J. Adams *et al.* (STAR Collaboration), J. Phys. G **32**, L37 (2006).

[37] J. Adams *et al.* (STAR Collaboration), J. Phys. G **34**, 451 (2007).

[38] H. Agakishiev *et al.* (STAR Collaboration), Phys. Lett. B **704**, 467 (2011).

[39] R. J. Glauber in *Lectures in Theoretical Physics*, edited by W. E. Brittin and L. G. Dunham (Interscience, New York, 1959), Vol. 1, p. 315.

[40] W. Czyż and L. C. Maximon, Ann. Phys. (NY) **52**, 59 (1969).

[41] A. Białas, M. Błeszyński, and W. Czyż, Nucl. Phys. B **111**, 461 (1976).

[42] A. Białas, J. Phys. G **35**, 044053 (2008).

[43] S. Eremin and S. Voloshin, Phys. Rev. C **67**, 064905 (2003).

[44] P. K. Netrakanti and B. Mohanty, Phys. Rev. C **70**, 027901 (2004).

[45] G. Agakishiev *et al.* (STAR Collaboration), Phys. Rev. C **86**, 014904 (2012).

[46] S. S. Adler *et al.* (PHENIX Collaboration), Phys. Rev. C **89**, 044905 (2014).

[47] C. Loizides, J. Nagle, and P. Steinberg, SoftwareX **1**, 13 (2015).

[48] A. Adare *et al.* (PHENIX Collaboration), Phys. Rev. C **93**, 024901 (2016).

[49] L. Zheng and Z. Yin, Eur. Phys. J. A **52**, 45 (2016).

[50] J. T. Mitchell, D. V. Perepelitsa, M. J. Tannenbaum, and P. W. Stankus, Phys. Rev. C **93**, 054910 (2016).

[51] C. Loizides, Phys. Rev. C **94**, 024914 (2016).

[52] A. Białas and A. Bzdak, Phys. Lett. B **649**, 263 (2007); Phys. Rev. C **77**, 034908 (2008)

[53] D. Kharzeev and M. Nardi, Phys. Lett. B **507**, 121 (2001).

[54] B. B. Back *et al.* (PHOBOS Collaboration), Phys. Rev. C **65**, 031901(R) (2002).

[55] P. Bożek and I. Wyskiel-Piekarska, Phys. Rev. C **85**, 064915 (2012).

[56] J. L. Albacete and A. Soto-Ontoso, Phys. Lett. B **770**, 149 (2017).

[57] A. Kovner and U. A. Wiedemann, Phys. Rev. D **66**, 034031 (2002).

[58] W. Broniowski, M. Rybczyński, and P. Bożek, Comput. Phys. Commun. **180**, 69 (2009); M. Rybczyński, G. Stefanek, W. Broniowski, and P. Bożek, *ibid.* **185**, 1759 (2014).

[59] R. S. Bhalerao, J.-P. Blaizot, N. Borghini, and J.-Y. Ollitrault, Phys. Lett. B **627**, 49 (2005).

[60] B. Schenke, S. Jeon, and C. Gale, Phys. Rev. Lett. **106**, 042301 (2011).

[61] S. Borsanyi *et al.*, JHEP **11** (2010) 077.

[62] M. Chojnacki and W. Florkowski, Acta Phys. Pol. B **38**, 3249 (2007).

[63] P. Bożek, Phys. Rev. C **85**, 034901 (2012).

[64] F. Cooper and G. Frye, Phys. Rev. D **10**, 186 (1974).

[65] A. Kisiel, T. Tałuć, W. Broniowski, and W. Florkowski, Comput. Phys. Commun. **174**, 669 (2006).

[66] M. Chojnacki, A. Kisiel, W. Florkowski, and W. Broniowski, Comput. Phys. Commun. **183**, 746 (2012).

[67] C. Gale, S. Jeon, and B. Schenke, Int. J. Mod. Phys. A **28**, 1340011 (2013).

[68] U. Heinz and R. Snellings, Annu. Rev. Nucl. Part. Sci. **63**, 123 (2013).

[69] S. Jeon and U. Heinz, Int. J. Mod. Phys. E **24**, 1530010 (2015).

[70] P. Bożek, Nucl. Phys. A **956**, 208 (2016).

[71] A. Mazeliauskas and D. Teaney, Phys. Rev. C **93**, 024913 (2016).

[72] P. Bożek and W. Broniowski, Phys. Rev. Lett. **109**, 062301 (2012).